



Semiclassical simulation of photochemical reactions in condensed phase

Maurizio Persico*, Giovanni Granucci, Silvia Inglese, Teodoro Laino,
Alessandro Toniolo

Dipartimento di Chimica e Chimica Industriale, Università di Pisa, via Risorgimento 35, I-56126 Pisa, Italy

Accepted 4 February 2002

Abstract

We compare two strategies for the semiclassical simulation of photochemical reactions in condensed phase (solutes in liquids, impurities in solid matrices, adsorbates, or photoreactive units in biological environments). Both strategies are based on classical nuclear trajectories, with surface hopping to simulate nonadiabatic transitions. In the first approach we calculate electronic energies and couplings by *ab initio* methods for many nuclear geometries of the reactive system (the ‘solute’), and we fit the results by analytic functions of the internal coordinates. In the case of surface crossings it is mandatory to resort to a (quasi-)diabatic representation of the electronic states. A condensed state environment (the ‘solvent’) is described by ordinary molecular mechanics (MM), and the solute–solvent interactions can be state-specific. The other strategy is direct, i.e. it involves the calculation of electronic energies and wavefunctions at each integration step of a nuclear trajectory. The method we have implemented is based on semiempirical configuration interaction calculations with floating occupation SCF orbitals; within this approach we have developed a hybrid quantum mechanics/molecular mechanics (QM/MM) procedure to represent the solvent, which is here briefly described for the first time. While the intra- and intermolecular potentials for the solvent molecules are of MM type, the QM/MM interaction is introduced in the semiempirical electronic hamiltonian, so that it influences in a state-specific way electronic energies and wavefunctions. Applications of both approaches to photoreaction dynamics are briefly described.

© 2002 Elsevier Science B.V. All rights reserved.

Keywords: Condensed state photochemistry simulations; Semiempirical methods; Nonadiabatic dynamics; Surface hopping; Quantum mechanics/molecular mechanics hybrid methods

1. Introduction

Most photochemical reactions taking place in condensed phase are deeply affected by interactions with the surrounding liquid or solid matrix. This is

important for well-known laboratory reactions normally performed in a variety of solvents, for photobiochemistry and even for heterogeneous photochemistry of importance in the atmosphere. The effects of the chemical environment may be classified as static or dynamic [1–4]. The former can be seen as deformations of the potential energy surfaces (PES) with respect to the isolated reactive system, resulting

* Corresponding author. Tel.: +39-050-918243; fax: +39-050-918260.

E-mail address: mau@dccl.unipi.it (M. Persico).

in spectral shifts and alteration in the height of energy barriers and accessibility of funnels in the excited states. Dynamical effects include all kinds of energy transfer to the environment, either in the excited or in the ground state, and the hindrance of large amplitude motions, such as the caging of photofragments.

Environmental effects on excited state energies can be theoretically evaluated by continuous models of the solvent [5]. Computational simulations of the photoreaction dynamics may take into account solute–solvent energy transfer by a simplified treatment based on Langevin dynamics [4]. However, a full treatment of both static and dynamical effects requires the inclusion of at least several of the molecules surrounding the reactive species, in order to take into account their mutual interactions, structural relationships, energy accepting capabilities and inertial properties. In this paper we compare two strategies we have implemented and applied to the mechanistic study of photochemical reactions: one requires the preliminary *ab initio* calculation of quasi-adiabatic electronic states and an analytic fit of the electronic quantities as functions of the internal coordinates [8,9], and the other one consists of the direct calculation of the nonadiabatic dynamics with ‘on the fly’ evaluation of the PES by semiempirical methods [10]. Both strategies are based on a semiclassical approach (nuclear trajectories plus surface hopping), but the latter has been also conjugated with the multiple spawning method by Martinez and coworkers [11].

Section 2 of this paper contains a brief outline of the general features which are common to both approaches. Section 3 is devoted to the first strategy (*ab initio* calculations and fit), with an example of application to the photolysis of azomethane. Section 4 describes the direct strategy and some preliminary results concerning the photolysis of ClOOCl adsorbed on an ice surface.

2. Semiclassical simulations of photochemistry: our options

The semiclassical approach to the simulation of the photochemical behavior of molecular systems consists of the classical treatment of the nuclear motion coupled with a quantum mechanical representation of

the electrons by a time-dependent wave function. There are a variety of semiclassical models, mainly differing in the coupling of the classical and quantum mechanical degrees of freedom [12–16]. In this section we briefly outline our basic options.

Each of the nuclear trajectories runs on a given adiabatic PES, but may jump to another PES at any time; the possibility of ‘surface hoppings’ provides the link between the two physical descriptions, classical and quantum mechanical. The electronic wavefunction $\Psi(t)$ evolves in time according to the time-dependent Schrödinger equation (TDSE):

$$i \frac{d}{dt} |\Psi(t)\rangle = \hat{\mathcal{H}}_{\text{el}}(t) |\Psi(t)\rangle \quad (1)$$

$\Psi(t)$ can be expanded on the basis of the N lowest adiabatic states ψ_K or in the equivalent diabatic basis $\{\eta\}$:

$$|\Psi(t)\rangle = \sum_K A_K(t) |\psi_K\rangle = \sum_I D_I(t) |\eta_I\rangle \quad (2)$$

$P_K(t) = |A_K|^2$ are the adiabatic probabilities; switching from an adiabatic surface to another depends on the $P_K(t)$ probabilities, according to Tully’s surface hopping algorithm [12]. However, the integration of the TDSE is more conveniently done by the diabatic expansion. In fact, the diabatic representation allows the simulation of the non-adiabatic dynamics in presence of quasidegenerate situations (weakly avoided crossings, conical intersections), where any approximate solution of the Schrödinger equation based on the adiabatic expansion is liable of inaccuracy. The $\{\eta\}$ and $\{\psi\}$ sets are connected by a unitary transformation ($\{\eta\} \mathbf{T} = \{\psi\}$), so the A_K coefficients are easily computed from the D_I ($\mathbf{A} = \mathbf{T}^{-1} \mathbf{D}$).

Swarms of trajectories are usually run, with initial conditions sampled according to Wigner or Boltzmann distributions in the ground state. In the former case one tries to reproduce the behavior of a quantum-mechanical wavepacket, while the Boltzmann distribution takes into account temperature effects in a classical approximation. The Boltzmann distribution can be obtained by running Langevin dynamics for a sufficiently long time [4]. Each trajectory starts with a vertical excitation to an electronic state chosen in a given excitation energy range, with a probability proportional to the oscillator strength of the transition.

The statistical analysis of the results eventually allows to extract several observables, such as quantum yields, final electronic states, fragment velocity distributions and anisotropies.

3. The traditional stepwise strategy

The standard simulation procedure, based on the Born–Oppenheimer scheme, goes through three steps. First of all, the calculation of ab initio adiabatic PES and couplings is needed for a large number of nuclear geometries. The results are then represented analytically by some kind of interpolation or fitting technique. The last step consists in computing the excited state dynamics by the semiclassical method described above.

The second step of the procedure must be modified if conical intersections or avoided crossings are present. In these regions, indeed, the adiabatic states may undergo abrupt changes, giving rise to sharp peaks or divergences in the nonadiabatic couplings and cusps in the PES.

To facilitate the fitting of the PES and the calculation of the dynamical couplings we would rather fit the electronic hamiltonian elements in the diabatic basis: $H_{IJ}^{\text{dia}} = \langle \eta_I | H_{\text{el}} | \eta_J \rangle$. The diabatic states $|\eta_I\rangle$ are defined so as to cancel, or at least minimize, the nonadiabatic or dynamical couplings $\langle \eta_I | \partial / \partial R_\alpha | \eta_J \rangle$, where R_α is an internal coordinate. This implies that their physical character changes, at most, very smoothly with the molecular geometry. Several operative definitions for the determination of (quasi-)diabatic states have been given [6–8]. Nearly all of them imply a rotation of the adiabatic basis to yield an orthogonal diabatic set $\{\eta\}$ spanning the same subspace, and the diabatic hamiltonian matrix \mathbf{H}^{dia} . When performing the simulations, the adiabatic energies and the approximate nonadiabatic couplings are easily computed by diagonalization of \mathbf{H}^{dia} .

3.1. Condensed state dynamics

The application of the standard simulation procedure to condensed state dynamics [17,19] requires to partition the system into a reactive core and an environment, which will be designed for brevity as

‘solute’ and ‘solvent’, respectively. Notice, however, that the computational schemes described in the following are suitable to represent also photochemical processes for adsorbates on a solid surface, molecules surrounded by a solid matrix, or chromophores in a biological environment. The classical dynamics of the solute’s nuclei is carried out with PES which include solvent–solvent and solute–solvent interaction potentials, in addition to the energy of the isolated molecule.

The solvent intra- and intermolecular potentials are taken from standard molecular mechanics (MM) models. The solute–solvent interaction may be modulated with reference to ab initio calculations of the solute plus solvent supermolecule, in order to take into account the state specificity of the solute–solvent interactions. We define a new diabatic hamiltonian matrix including the solute–solvent interactions \mathbf{V}_{solv} :

$$\mathbf{H}_{\text{sol}}^{\text{dia}} = \mathbf{H}^{\text{dia}} + \mathbf{V}_{\text{solv}}. \quad (3)$$

\mathbf{V}_{solv} is expressed in the diabatic basis in order to have a more regular dependence of the interaction with the nuclear coordinates. We underline the importance of adding \mathbf{V}_{solv} before the diagonalization of \mathbf{H}^{dia} if one wants to take into account state specific solute–solvent interactions. In fact, the interaction depends on the electronic wavefunction of the solute (polarizability, charge distribution, etc.) and the wavefunction is in turn influenced by solvent effects, therefore, it is not rigorously correct to modify the K th adiabatic PES with the corrective term $\langle \psi_K | V_{\text{solv}} | \psi_K \rangle$, where ψ_K has been determined for the isolated molecule.

A simple model of avoided crossing shows that a direct modification of the adiabatic PES may lead to unphysical features. Fig. 1 shows two adiabatic potential energy curves versus an internal coordinate, obtained by diagonalization of a 2×2 hamiltonian matrix: H_{11} and H_{22} are a Morse function and a repulsive exponential, respectively, and H_{12} is constant. In the upper panel, we add two different constant corrections V_1 and V_2 to the diagonal matrix elements, to simulate solute–solvent interactions, and we show the resulting eigenvalues of the modified matrix. The avoided crossing is shifted along both the energy and coordinate axes. In the lower panel, we add to each eigenvalue E_K of the unperturbed \mathbf{H}^{dia}

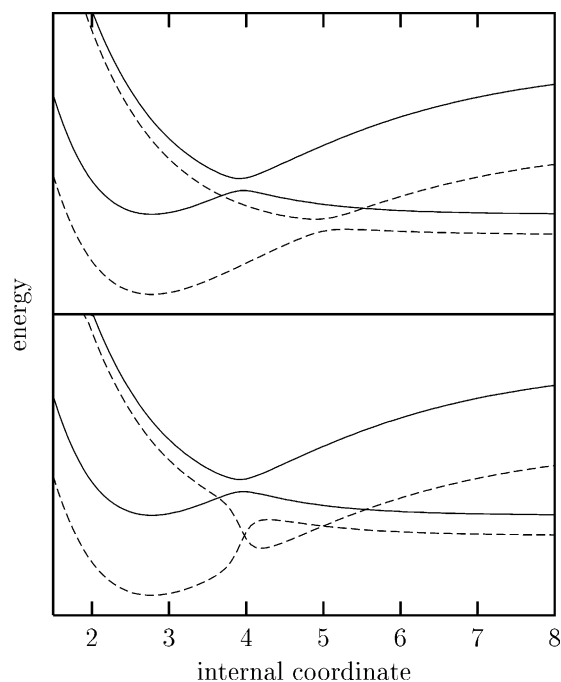


Fig. 1. Model of avoided crossing with solute-solvent interactions. Full lines: unperturbed adiabatic potential energy curves for the isolated solute, computed as eigenvalues of a hypothetical diabatic hamiltonian matrix (same in the upper and lower panels). Dashed lines: potential energies taking into account state-specific solvent effects. In the upper panel, the perturbation due to the solvent is added to the diagonal matrix elements of the diabatic hamiltonian, which is then diagonalized. In the lower panel, the adiabatic energies computed for the isolated molecule are corrected by addition of the expectation values of the solute-solvent interaction (see text). Arbitrary units.

matrix the corresponding expectation value $T_{K1}^2 V_1 + T_{2K}^2 V_2$, where T_K is an eigenvector of H^{dia} . This procedure yields an unphysical double crossing, which is reminiscent of similar artifacts previously analyzed by Spiegelmann and Malrieu in connection with perturbative corrections of configuration interaction (CI) energies [18].

3.2. Simulations of the photochemistry of azomethane

The computational approach outlined in the preceding sections has been applied to a study of the photolysis of azomethane, $\text{CH}_3\text{-N=N-CH}_3$, both in vacuo and in water solution [19]. The quasi-diabatic PES and couplings were computed

by multireference perturbation CI and fitted with a rather elaborated analytic function of the internal coordinates, taking into account the symmetry of the nonrigid molecule [20]. In vacuo, the $n \rightarrow \pi^*$ excited state rapidly decays by internal conversion to the ground state, with a lifetime of about 0.5 ps. In fact, the minimum energy path in the $n \rightarrow \pi^*$ PES implies torsion about the N=N double bond and, for $\angle \text{CNNC} \approx 90^\circ$, is very close to a crossing seam between the two surfaces. A minor fraction of $\text{CH}_3\text{NN}\cdot + \text{CH}_3\cdot$ radicals (10–20%) are produced by prompt dissociation, within 1 ps, partly in the excited state surface, the importance of this process increases with the photon energy. Most of the dissociation takes place with longer times (> 100 ps), after the molecule has settled either in the *cis* or in the *trans* minimum by distributing the vibrational energy among all vibrational modes. The dissociation of the second N-C bond follows in a short time (≈ 10 ps), leading to $\text{N}_2 + 2\text{CH}_3\cdot$. The simultaneous dissociation of both N-C bonds also occurs, but with very low probability (about 7% of the trajectories). These findings allowed us to interpret and to solve the apparent contradiction between the experimental results of Lee's [21] and Zewail's [22] groups, who found evidence of slow and fast dissociation, respectively.

For the simulation of photolysis in aqueous solution, we adopted the flexible SPCE model of water [23,24], and we imposed periodic boundary conditions with a unit cell containing 120 molecules of water and one of azomethane. For the sake of simplicity, in that work we did not consider state specific solute-solvent interactions; we adopted Lennard-Jones potentials between C, N and H of azomethane and the water oxygen, with the same parameters for ground and excited state. The simulations show that the short time dynamics is the same in vacuo and in solution; the internal conversion to the ground state and the isomerization take approximately the same time. Only the fast dissociation of the N-C bond is almost completely suppressed. On an intermediate time scale, the energy transfer to the solvent is important. The vibrational temperature of azomethane decreases almost exponentially, with a time constant of about 16 ps; the cooling becomes slower at still longer times. The latter observation can be interpreted as

a consequence of the internal energy redistribution of the solute. In fact, immediately after the excitation and the internal conversion, most of the vibrational energy is stored in low frequency, large amplitude, internal motions, such as double bond torsion, N-inversion and NC bond elongation, which are more effective in transferring energy to the solvent. The cooling of azomethane competes successfully with dissociation, which is quite effectively inhibited; only isomerization is observed, in agreement with the experimental observations. This typical example of cage effect is only marginally due to a real hindrance of the separation of two photodissociated fragments. The main mechanism is simply vibrational quenching in the ground state.

4. The ‘direct’ strategy

The direct strategy for the simulation of excited state dynamics is based, as the ‘standard’ one, on the semiclassical approach; the nuclei are treated as classical particles while the electrons are quantum mechanical. The PES and their gradients, which govern the nuclear motion, as well as the electronic wavefunctions, are calculated on the fly, by solving at each trajectory integration step the time independent Schrödinger equation for the electrons at fixed nuclei. The direct approach is more easily applied to semiclassical dynamics than to quantum wavepacket dynamics, owing to the delocalized nature of the latter. Past attempts using *ab initio* methods to solve the electronic problem faced rather severe limitations, due to the very high number of calculations one needs to perform and to the exacting requirements for accurate excited state calculations [11,25,26]. Other strategies, using the empirical VB [27] or the diatomics-in-molecules methods [14] are computationally much less demanding. These approaches may be qualified as ‘direct’, in that they imply a quantum mechanical treatment of the electronic problem, although simplified. Notice, however, that the empirical hamiltonians are defined by fitting experimental or *ab initio* data.

The method we employ to calculate the electronic states is semiempirical, of the NDO type; the electronic wave functions are of the CI type, with molecular orbitals (MO) obtained in a SCF

calculation with fractional, and possibly variable (‘floating’), occupation numbers. This choice ensures a correct treatment of homolytic dissociations and of the fragment orbital degeneracy, and a partial optimization of the virtual orbitals. An SCF with fractional occupation is performed as a closed shell one, including arbitrary occupation numbers N_k in the density matrix ρ definition:

$$\rho_{ij} = \sum_k N_k C_{ik} C_{jk}. \quad (4)$$

Some of the orbitals may have $N_k = 2$ or $N_k = 0$, and not to be active in the CI, so as to reduce the cost of the CPHF procedure for energy derivatives. The other occupation numbers may be either arbitrarily fixed or floating. In the latter case, the N_k values are self-consistently determined according to the orbital energies ε_k

$$N_k = \frac{\sqrt{2}}{\sqrt{\pi}w} \int_{-\infty}^{\varepsilon_F} \exp\left[-\frac{(\varepsilon - \varepsilon_k)^2}{2w^2}\right] d\varepsilon \quad (5)$$

where ε_F is the Fermi level, adjusted so that $\sum_k N_k$ is the total number of electrons, and w is an arbitrarily chosen orbital energy width parameter, which determines the spread of electronic populations below and above the Fermi level. Most semiempirical parametrizations were optimized within the closed shell SCF approximation for the ground state. Therefore, the standard parameters may not be optimal for a CAS-CI with floating occupation of the MOs and a modification may be necessary. Consequently, after we have defined a minimal MO active space for the CAS-CI calculation, sufficient to represent all the electronic states along the reaction pathways of interest, and chosen the MO energy width w in order to achieve easy convergence of the SCF process at all geometries, it will be important to recalibrate some or all of the semiempirical parameters, with the goal of reproducing experimental or *ab initio* results for the particular system under study [28]. These new features have been implemented in a development version of the MOPAC package [29].

As we have already observed, the integration of the TDSE in the adiabatic representation is liable to inaccuracy in case of weakly avoided curve crossings or in the proximity of conical intersections. Therefore, we resort to a ‘locally diabatic’ representation to make our algorithm inherently stable in such cases.

The diabatic states are obtained by rotation of the adiabatic basis, according to the overlaps $\langle \psi_k(t) | \psi_k(t + \Delta t) \rangle$, computed across a time-step: therefore, they are diabatic only with regard to a given trajectory [10].

4.1. QM/MM procedure

The presence of a condensed phase (the solvent) interacting with the photoreactive system (the solute) will be again simulated by MM. Since the electronic degrees of freedom of the solute are treated by a quantum mechanical method, we set up a mixed quantum mechanics (QM)/MM procedure. As in the ‘traditional’ strategy (Section 3.1), it is important that the solute–solvent interactions are added to the QM hamiltonian, so that they affect in a correct way the solute electronic energies and wavefunctions. In the present implementation of the method, only the electrostatic interactions are treated in this way, and are therefore state-specific. Other terms, such as dispersion–repulsion, are simply added to the total energy in the form of Lennard–Jones 6–12 atom–atom potentials, so they must be the same for all electronic states. The electrostatic part of the QM/MM hamiltonian is

$$\hat{\mathcal{H}}^{(\text{QM/MM})} = \sum_{\alpha} \sum_{\beta} \frac{Z_{\alpha} Z_{\beta}}{R_{\alpha\beta}} - \sum_i \sum_{\beta} \frac{Z_{\beta}}{R_{i\beta}} \quad (6)$$

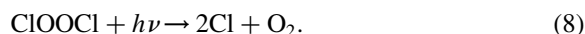
where α and i number the nuclei and electrons of the solute, and β the atoms of the solvent, carrying the charge Z_{β} .

Given the semiempirical simplification of the interaction hamiltonian, only one-center integrals are involved; once the sum over the index β is done, we are left with 10 independent one-electron integrals $h_{\mu\nu}^{(\text{QM/MM})} = \langle \mu | Z_{\beta} / R_{i\beta} | \nu \rangle$ for each atom of the solute with an sp shell (but only one for the hydrogen atoms). The $h_{\mu\nu}^{(\text{QM/MM})}$ integrals depend on the positions of all the solvent atoms. So, taking for instance a solute with four heavy atoms and six hydrogens (azomethane), and 200 water molecules, the number of cartesian coordinates is: (solvent atoms + solute atoms) \times 3 = (200 \times 3 + 10) \times 3 = 1830. We do not need to calculate 1830 CI energy derivatives, each time repeating the CPHF procedure. We calculate instead the CI energy derivatives with

respect to the $h_{\mu\nu}^{(\text{QM/MM})}$ parameters, whose number is: (solute heavy atoms) \times 10 + (solute hydrogens) = 46. With the chain rule we get all the 1800 derivatives with respect to solvent atom coordinates. Thirty more derivatives with respect to solute atom coordinates are made in the usual way.

4.2. ClOOCl photodissociation

The ClO dimer plays an important role in the antarctic ozone hole formation, because it is an intermediate in the reversion of ClO radicals to Cl atoms:



The photodissociation may occur stepwise:



A competing process, which generates a null cycle, is:



We have simulated the photodissociation of an isolated ClOOCl molecule by the direct strategy, using a reparametrized MNDO/d hamiltonian [30]. The computed quantum yields and final fragment energies agree with those measured by [28]. Moore et al. [31]. Little ClO is produced, and only for $h\nu > 4.5$ eV, at the upper end of the explored photon energy range (2.2–5.0 eV). The photodissociation to $2\text{Cl} + \text{O}_2$ mainly follows the stepwise mechanism at low photon energies, and the simultaneous Cl–O bond breaking at high energies.

The surface of ice particles in the polar stratospheric clouds may accelerate the dimerization reaction (8), and/or adsorb ClOOCl. Adsorption may affect the photochemistry of ClOOCl in several ways: (a) by causing spectral shifts and changes in the photoabsorption cross sections; (b) by altering the relative yields of 2ClO and $2\text{Cl} + \text{O}_2$; (c) by inhibiting the photodissociation due to energy transfer to ice and/or desorption; (d) by further interaction of the photodissociation products with the ice surface.

In order to investigate the photolysis of adsorbed ClOOCl, we have prepared the ClOOCl–ice system in three steps: (1) optimize a cluster of 216 water

molecules (flexible SPC model) in three layers, with periodic geometry constraints corresponding to the Ih crystal structure; (2) fix the position of all atoms in the bottom layer and at the borders, and optimize the remaining 64 water molecules without other constraints; (3) add ClOOCl on top and re-optimize the

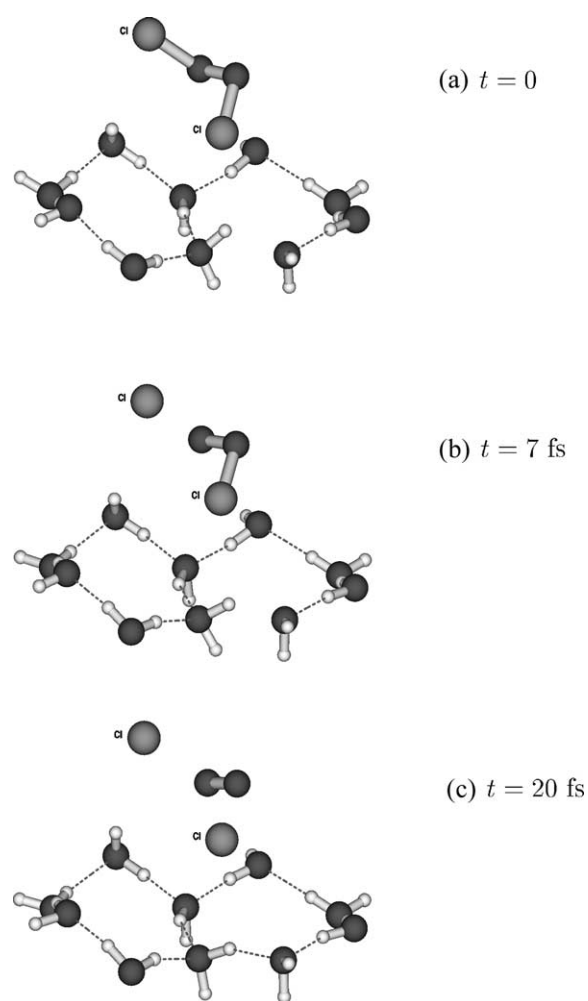


Fig. 2. (a) ClOOCl and the 10 closest water molecules belonging to the ice surface at the beginning of a semiclassical trajectory (time $t = 0$). The distance between the foremost Cl and H atoms is 2.89 Å. (b) Same as (a), at $t = 7$ fs after the excitation. One of the Cl–O distances has started to increase (from its initial value, 1.97 Å, to 2.07 Å). The other Cl–O distance is practically constant. (c) Same as (a), at $t = 20$ fs after the excitation. Also the second Cl–O distance has now increased, from 1.92 to 2.11 Å, while the first is now 2.50 Å. The H atom to which Cl was more strongly bound is now rotating so as to form another bond with the nearest water oxygen.

constrained ice slab plus adsorbate with the QM/MM procedure outlined in the preceding section. When running the semiclassical dynamics, only the 64 free water molecules can move.

Only preliminary results for the photodissociation dynamics are available: they concern the lowest range of photon energies (2.2–3.4 eV). Initially ClOOCl is bound to one or two water molecules through the Cl atoms, as shown in Fig. 2a. Most of the trajectories show a stepwise dissociation. The Cl atoms and the ClOO radicals are still bound to ice after the first bond breaking, while the O₂ molecules tend to fly away (see Fig. 2b and c, representing two snapshots of a typical trajectory). No desorption of ClOOCl as a whole occurs. About 0.5 eV of the available energy are transferred to ice in the form of vibrational energy and deformations of the ice lattice.

5. Conclusions

We have presented two semiclassical approaches to nonadiabatic excited state dynamics, which may qualified as ‘stepwise’ and ‘direct’, respectively. Both have already been applied to simulate photochemical reactions in vacuo as well as in a condensed phase.

The main effort in the stepwise procedure is put in computing ab initio electronic energies and wavefunctions for many geometries, and in finding suitable fitting functions. The presence of surface crossings and the introduction of state specific solute–solvent interactions require the definition of quasi-diabatic electronic states, which is not a trivial task for polyatomics with multiple reaction channels [8]. Once the hamiltonian matrix elements in the diabatic basis have been expressed as analytic functions, running the semiclassical simulations is usually a less time-consuming step. Therefore, one can easily compute many trajectories, in order to have a good statistical basis for the analysis of the results, and possibly repeat the simulation with different methods and options. Relatively long simulations can be afforded (for instance, we went up to 500 ps for azomethane in vacuo).

The direct strategy has been devised to avoid the cumbersome task of building the PES (either in the diabatic or in the adiabatic representation), and to deal with large molecular systems, for which the ab initio

calculations are unpractical. Of course, an extensive reparametrization of the semiempirical method may require some care and is often partly based on ab initio results, for lack of experimental data on some portions of the PES. However, semiempirical methods can usually be trusted to yield sufficiently accurate results for all parts of the molecule not directly involved in the chromophore, yet being important for the reaction dynamics. Running semiclassical dynamics with a direct approach is computationally more demanding, so the efficiency of the method depends, among other things, on the trajectory integration procedure and on the algorithm for the calculation of the CI energy gradients [32,33]. A QM/MM approach is the best way to represent the effect of the chemical environment. With respect to the simple version we have implemented so far, the most important improvement will be to introduce the representation of covalent bonding between the QM and MM subsystems, which is necessary to treat chromophores bound to biological or synthetic polymer matrices. The dielectric properties of the medium would be more realistically accounted for by defining variable (instead of fixed) atomic charges, and/or by coupling the explicit representation of a number of solvent molecules with a continuum dielectric [5] extending to infinite distance from the reactive system. Such are the developments we foresee in the near future.

References

- [1] J.T. Hynes, R. Kapral, G.M. Torre, *J. Chem. Phys.* 72 (1980) 177.
- [2] P.A. Rejto, E. Bindewald, D. Chandler, *Nature* 375 (1995) 129.
- [3] T. Sakka, K. Matsumara, T. Tsuboi, Y.H. Ogata, *Chem. Phys. Lett.* 286 (1998) 107.
- [4] P. Cattaneo, G. Granucci, M. Persico, *J. Phys. Chem. A* 103 (1999) 3364.
- [5] C. Amovilli, V. Barone, R. Cammi, E. Cancès, M. Cossi, B. Mennucci, C.S. Pomelli, J. Tomasi, *Adv. Quantum Chem.* 32 (1998) 227.
- [6] T. Pacher, L.S. Cederbaum, H. Köppel, *Adv. Chem. Phys.* 84 (1993) 293.
- [7] M. Persico, Electronic diabatic states: definition, computation and applications, in: P.v.R. Schleyer, N.L. Allinger, T. Clark, J. Gasteiger, P.A. Kollman, H.F. Schaefer III, P.R. Schreiner (Eds.), *Encyclopedia of Computational Chemistry*, Wiley, Chichester, 1998, p. 852.
- [8] P. Cattaneo, M. Persico, *Chem. Phys.* 214 (1997) 49.
- [9] P. Cattaneo, M. Persico, A. Tani, *Chem. Phys.* 246 (1999) 315.
- [10] G. Granucci, M. Persico, A. Toniolo, *J. Chem. Phys.* 114 (2001) 10608.
- [11] M. Ben-Nun, J. Quenneville, T.J. Martinez, *J. Phys. Chem. A* 104 (2000) 5161.
- [12] J.C. Tully, *Int. J. Quantum Chem.* S 25 (1991) 299.
- [13] W. Domcke, G. Stock, *Adv. Chem. Phys.* 100 (1997) 1.
- [14] A. Bastida, F.X. Gadéa, *Z. Phys. D* 39 (1997) 325.
- [15] M.S. Topaler, T.C. Allison, D.W. Schwenke, D.G. Truhlar, *J. Chem. Phys.* 109 (1998) 3321.
- [16] Y.L. Volobuev, M.D. Hack, D.G. Truhlar, *J. Phys. Chem. A* 103 (1999) 6225.
- [17] P. Cattaneo, M. Persico, A. Tani, *Chem. Phys.* 246 (1999) 315.
- [18] F. Spiegelmann, J.-P. Malrieu, *J. Phys. B* 17 (1984) 1235.
- [19] P. Cattaneo, M. Persico, *J. Am. Chem. Soc.* 123 (2001) 7638.
- [20] P. Cattaneo, M. Persico, *Theor. Chem. Acc.* 103 (2000) 390.
- [21] A.S. Bracker, S.W. North, A.G. Suits, Y.T. Lee, *J. Chem. Phys.* 109 (1998) 7238.
- [22] E.W.-G. Diau, O.K. Abou-Zied, A.A. Scala, A.H. Zewail, *J. Am. Chem. Soc.* 120 (1998) 3245.
- [23] H.J.C. Berendsen, J.R. Grigera, T.P. Straatsma, *J. Phys. Chem.* 91 (1987) 6269.
- [24] J. Martí, E. Guàrdia, J.A. Padró, *J. Chem. Phys.* 101 (1994) 10883.
- [25] T. Vreven, F. Bernardi, M. Garavelli, M. Olivucci, M.A. Robb, H.B. Schlegel, *J. Am. Chem. Soc.* 119 (1997) 12687.
- [26] A.L. Kaledin, K. Morokuma, *J. Chem. Phys.* 113 (2000) 5750.
- [27] S. Clifford, M.J. Bearpark, F. Bernardi, M. Olivucci, M.A. Robb, B.R. Smith, *J. Am. Chem. Soc.* 117 (1995) 27.
- [28] G. Granucci, A. Toniolo, *Chem. Phys. Lett.* 325 (2000) 79.
- [29] J.J.P. Stewart, *MOPAC 2000*, Fujitsu Limited, Tokyo, Japan, 1999.
- [30] A. Toniolo, G. Granucci, S. Inglese, M. Persico, *PCCP* 3 (2001) 4266.
- [31] T.A. Moore, M. Okomura, J.W. Seale, T.K. Minton, *J. Phys. Chem.* 103 (1999) 1691.
- [32] P. Patchkovski, W. Thiel, *Theor. Chem. Acc.* 98 (1997) 1.
- [33] R. Izzo, M. Klessinger, *J. Comput. Chem.* 21 (2000) 52.